HHS Public Access

Author manuscript

ACS Chem Neurosci. Author manuscript; available in PMC 2019 April 17.

Published in final edited form as:

ACS Chem Neurosci. 2018 December 19; 9(12): 3072–3085. doi:10.1021/acschemneuro.8b00284.

Structural Analysis of Hippocampal Kinase Signal Transduction

Daniel B. McClatchy[1], **Nam-Kyung Yu**[1], **Salvador Martínez-Bartolomé**[1], **Reesha Patel**[2], **Alexander R. Pelletier**[3], **Mathieu Lavalle-Adam**[3], **Susan B. Powell**[4], **Marissa Roberto**[2], and **John R. Yates**[*,1]

[1]Department of Molecular Medicine, The Scripps Research Institute, La Jolla, CA, USA

[2]Department of Neuroscience, The Scripps Research Institute, La Jolla, CA, USA

[3]Department of Biochemistry, Microbiology and Immunology and Ottawa Institute of Systems Biology, University of Ottawa, Ottawa, ON, CAN

[4]Department of Psychiatry, UCSD, La Jolla, CA, USA

Abstract

Kinases are a major clinical target for human diseases. Identifying the proteins that interact with kinases *in vivo* will provide information on unreported substrates and will potentially lead to more specific methods for therapeutic kinase regulation. Here, endogenous immunoprecipitations of evolutionally distinct kinases (i.e. Akt, ERK2, and CAMK2) from rodent hippocampi were analyzed by mass spectrometry to generate three highly confident kinase protein-protein interaction networks. Proteins of similar function were identified in the networks, suggesting a universal model for kinase signaling complexes. Protein interactions were observed between kinases with reported symbiotic relationships. The kinase networks were significantly enriched in genes associated with specific neurodevelopmental disorders providing novel structural connections between these disease-associated genes. To demonstrate a functional relationship between the kinases and its network, pharmacological manipulation of Akt in hippocampal slices was shown to regulate the activity of potassium/sodium hyperpolarization-activated cyclic nucleotide-gated channel(HCN1), which was identified in the Akt network. Overall, the kinase protein-protein interaction networks provide molecular insight of the spatial complexity of *in vivo* kinase signal transduction which is required to achieve the therapeutic potential of kinase manipulation in the brain.

Keywords

kinase; mass spectrometry; hippocampus; protein-protein interactions; HCN1; Akt

[*]corresponding author.

Authors Contributions

D.B.M., J.R.Y., R.P., S.B.P., and M.R. designed the experiments, D.B.M., N.Y., R.P., and S.B.P. performed the experiments, D.B.M., S.M., A.R.P. and M.L. analyzed the data, and D.B.M. wrote the manuscript.

Supplementary Data

Our proteomic data can be viewed and queried at http://sealion.scripps.edu/pint/?project=8b08244cc5fb0b2ee5532285bce8b7f6 which is also linked to additional data analysis tools for further investigation. The MS raw files have been uploaded to ProteomeXchange (PXD009871).

Introduction

Information or signals can travel through a cell via reversible protein phosphorylation. The addition of a phosphate group can produce different biochemical outcomes including altering a protein's activity, subcellular localization, or interactions. Over 500 genes in the human genome are annotated as kinases, which are the enzymes that catalyze the addition of a phosphate group onto a protein substrate. Structurally, kinases possess a non-conserved regulatory domain and a conserved catalytic domain. They can be simply categorized by whether they phosphorylate serine/threonine residues or tyrosine residues, but a more detailed classification based on sequence alignment of the catalytic domains separates the kinases into nine broad groups comprising hundreds of gene families [1]. Decades of extensive research have identified a plethora of substrate-kinase relationships that are vital in cellular homeostasis to direct the flow of information through a signaling pathway. This research has demonstrated that kinases can have a preferred amino acid (AA) sequence (i.e. phospho-motif) that surrounds the phosphorylated residue [2]. There is also evidence that many substrates can be phosphorylated regardless of the surrounding AA residues, suggesting kinase promiscuity or possibly an additional three-dimensional structural requirement[3]. *In vivo* kinase signaling seems to be staggeringly complex with many molecular details poorly understood. Many well-studied kinases have hundreds of identified substrates and based on the number of phosphorylated residues that have been identified in the entire proteome, there are probably even more unidentified substrates [4]. These substrate-kinase relationships become further convoluted by reports that multiple kinases can phosphorylate the same substrate and the activity of a kinase itself can be regulated by phosphorylation. This implies that *in vivo* phosphorylation signaling cannot be represented by a simple linear kinase-substrate pathway. This communication between different kinase signaling pathways has been described as "cross-talk" and could be a mechanism to fine tune a biological response to multiple extracellular perturbations. Understanding this signaling complexity is vital, as aberrant phosphorylation and mutated kinases have been demonstrated to cause or contribute to a large variety of human diseases. Thus, kinases are a promising drug target for potential cures and therapies[5].

Beyond the identification of substrates, it is unclear how soluble kinases navigate through a complex proteome to phosphorylate the appropriate substrate at the appropriate time. One hypothesis is that additional proteins, described as adaptor or scaffolding proteins, organize signaling complexes to increase the kinetics of the kinase reaction with low abundant substrates. In yeast, Ste5 facilitates kinase signaling by serving as a scaffold for the yeast MAPK (mitogen-activated protein kinase) signaling pathway. This pathway is defined by the classical three kinase cascade in which Ste11p kinase activates its substrate, Ste7p kinase, which then phosphorylates and activates Fus3p kinase. Ste5 coordinates this signaling network by interacting with all three kinases via three different binding domains[6]. In mammalian cells, scaffolding proteins have been identified for PKA (Protein Kinase A) and PKC (Protein Kinase C) serine/threonine kinase families. The AKAPs (A-Kinase Anchoring Proteins) are scaffolding proteins that bind and anchor PKA at optimal subcellular localizations to facilitate the phosphorylation of its substrates[7]. Similarly, different RACK (receptors for activated C kinase) proteins have been reported to bind specific PKC isozymes

and their substrates to specific subcellular compartments, which increases the PKC phosphorylation of these substrates[8]. Further studies have demonstrated both RACKs and AKAPs bind and regulate many proteins outside the canonical PKC and PKA signaling pathways, including tyrosine kinases, other serine/threonine kinases, phosphatases, phosphodiesterases and cytoskeletal proteins to form multifunctional signaling complexes [9, 10]. Importantly, many laboratories have exploited the scaffolding protein structure to manipulate kinase signaling suggesting they are another potential avenue for therapeutic kinase regulation[11].

Kinase signaling complexes may be the most critical in the brain, because it is the tissue with the highest levels of phosphorylation[12]. The hippocampus, which is essential for learning and memory, is the brain region with the highest expression of kinases and phosphatases and it contains the largest number of phosphorylated proteins [13]. This suggests that the hippocampus is an excellent resource to study the diversity of signaling complexes. Some signaling complexes that modulate hippocampal function have already been identified. AKAP5 binds PKA and the phosphatase calcineurin to anchor them to the post-synaptic density in the hippocampus to regulate the phosphorylation on serine 845(S845) of AMPAR (amino-3-hydroxy-5-methylisooxazole-4-propionic acid receptor) subunit GluR1. Manipulation of this AKAP5 complex alters synaptic plasticity, which is essential for learning and memory [14]. In hippocampal dysfunction, hyper-phosphorylation of the protein tau forms intracellular neurofibrillary tangles which are a key pathological determinant of Alzheimer's disease(AD) [15]. Therefore, analysis of signaling complexes can lead to a greater understanding of the biochemical underpinnings of hippocampal function and pathogenesis.

The identification of signaling complexes, however, is very limited compared to the hundreds of kinases in the human genome. To identify novel signaling complexes *in vivo*, mass spectrometry (MS) analysis was performed on endogenous kinase immunoprecipitations from the hippocampus to construct protein-protein interaction(PPI) networks. Arguably, majority of reported of PPIs are investigated using the overexpression of tagged proteins and then an antibody to the tag enriches the bait and its PPI network for MS analysis[16]. Although biological relevant PPIs have been discovered, there are disadvantages to this approach[17]. The tag amended to the protein may cause a structural change to the bait resulting in an altered PPI network. In addition, exogenous tagged protein is often over-expressed compared to the endogenous untagged protein, which can cause altered subcellular localization, spurious interactions, and cellular stress. The exogenous tagged protein also is competing with interactors with the endogenous untagged protein. Finally, it is very time consuming to generate transgenic animals for this approach for tissue analysis. For these reasons, enrichment of the endogenous kinase and its PPI network with an antibody was chosen for this study to obtain PPI networks closest to physiological conditions as possible. One caveat to both approaches is that an antibody may have off-target interactions. To control for these off-target interactions, the antibody enrichment is performed in biological sample without its antigen. This control is simple to perform with exogenous expressed tagged proteins with an antibody specific for the tag, but is more difficult and sometimes impossible with the immunoprecipitation of endogenous proteins from tissue. To help control for this potential problem, control IPs were performed with non-

specific IgGs. This study analyzed kinases from three structurally distinct kinase groups: Akt (also known as Protein Kinase B) from the AGC kinase group, CAMK2(Calcium/calmodulin dependent kinase type II) from the CAMK kinase group and ERK2(Extracellular signaling-Regulated Kinase 2 or also known as MAPK1) from the STE kinase group. These kinases have been reported to be crucial for hippocampal function and dysfunction, but global analysis of the PPIs of these kinases in the hippocampus has not been reported. Overall, this study reveals an unprecedent complexity in kinase signaling complex and novel insight into the consequences of pharmacological manipulation of kinases in the hippocampus.

Results and Discussion

Construction of highly confident Kinase PPI networks

To generate highly confident kinase PPI networks, hippocampi from six different rats were employed for each kinase. Each solubilized hippocampus was divided evenly for an immunoprecipitation(IP) with a kinase antibody or control IP with normal serum. Thus, there were 6 control IPs and 6 bait IPs for each kinase target. After protein digestion, each IP was analyzed by mass spectrometry(MS). Since kinases exist as groups of highly homologous gene families, the specific kinase isoform used to construct the network was first defined for each kinase IP-MS dataset. The Akt family consists of three isoforms (i.e. Akt1, Akt2, and Akt3) that share 80% AA homology and the antibody used in this study reacts with all three. All isoforms are expressed in the brain and it has been reported that in the hippocampus Akt3 is the most abundant, followed by Akt1 then Akt2[18]. When isoform specific peptides were examined in the Akt IP-MS data, a similar trend was observed with peptides unique to Akt3 having the highest spectra count(SC) (Figure 1A). SC is defined as the number of times the mass spectrometer identifies a peptide, and it correlates with abundance in the protein sample [19]. The ERK2 antibody employed in this analysis has been reported by the manufacturer to also react weakly with ERK1, which contains 80% AA homology with ERK2. When isoform specific peptides were examined in the ERK2 IP-MS data, 98% of the unique peptide abundance was attributed to ERK2(Figure 1B). In contrast to the single protein kinase activity of Akt and ERK2, CAMK2 is a dodecameric kinase complex composed of two hexameric kinase stacked rings[20]. The complex can be composed of different isoforms (i.e. alpha, beta, delta, and gamma) which share greater than 70% AA homology. The most abundant CAMK2 structure in the hippocampus consists of alpha and beta isoforms at a 3:1 ratio [21].

The CAMK2 antibody employed in this study has been reported by the manufacturer for use in detecting alpha, and it is predicted to react with delta and gamma, but not with the beta isoform. When isoform specific peptides were examined in the CAMK2 IP-MS data, 64% of the CAMK2 unique peptide abundance originated from the alpha isoform and 33% from the beta isoform. Only 3% of the unique peptide abundance originated from the gamma isoform and no unique peptides were observed for the delta isoform (Figure 1C). Based on this unique peptide evidence, Akt3, CAMK2A, and ERK2 were annotated as the bait kinases for subsequent bioinformatic analyses.

The bait kinases were shown to be enriched greater than 10-fold in the IP over starting material (hippocampal lysates) using MS analysis (Figure 1D). In the bait IP-MS data, approximately fifty percent of the identified proteins were identified in all six biological replicates, while most of the proteins identified in control IP-MS data were only identified in one replicate (Figure 1E). This suggests that the control IPs contain more non-specific interactions than the bait IPs. Although proteins that were identified consistently with the baits have high potential to be interactors, these proteins may also be contaminants or false positive interactors [22]. The algorithm SAINT was used to distinguish between the true and false interactors [23]. In this algorithm, the reproducibility and the abundance distribution of the potential interactors among the biological replicates is compared between the bait and control IP-MS datasets to assign a probability of each protein being a true interactor with the bait kinase. A 5% FDR filter was applied to the datasets which was equivalent to ~85% probability or greater that the identified protein is a true interactor according to the SAINT algorithm. Using this criterion, very stringent PPI networks are generated which consist of the top 10% most reproducible identifications with all these interactors being identified in every biological replicate (Figure 1F and TableS1).

In total, there were 59 unique interactors in the Akt3 network, 161 in the ERK2 network and 101 in the CAMK2A network. Most of the interactors were specific to one kinase PPI network, but there was some overlap, with the largest overlap occurring between ERK2 and CAMK2A (Figure 2A and TableS2). Using the IntAct database[24], previously reported interactions were identified. For example, ERK2 was identified previously in a purification of the post-synaptic protein PSD-95 (DLG4) from mouse brain and DLG4 was specifically associated with our ERK2 network[25]. In addition, protein isoforms of known interactors were identified. For example, CAMK2A has been reported to interact with the proteasome and multiple specific regulatory proteasome subunits[26]. In our CAMK2A network, regulatory subunit Proteasome 26S subunit ATPase 3 (PSMC3) was identified, but this subunit was not observed in the previous study. These known interactions constituted less than 5% of the interactions in our networks. Next, the STRING interaction database was used to determine if there were reported functional interactions between the proteins within a network[27]. The number of functional interactions identified within the networks varied considerably. While the Akt3 and CAMK2A networks had fewer than 40 STRING interactions, the ERK2 network had greater than 600, most of which originated from interactions between different ribosomal subunits.

Even after normalization to account for the size of the ERK2 network, the number of STRING interactions found in the ERK2 network was 10 times higher than in the other networks (Figure 2B and TableS3). Other than the ribosomal network, most known interactions identified were binary (Figure 2C, S1, and S2). For instance, Peroxin-5-related protein (Pex5l) has been reported to bind hyperpolarization-activated cyclic nucleotide-gated 1 channel (HCN1) to regulate its trafficking to the plasma membrane[28] and both HCN1 and Pex5l were identified in the Akt3 network. Identification of known interactions with the bait kinases and known interactions between network proteins confirms the high confidence of our kinase PPI networks.

Synaptic Proteins and Pathways enriched in the PPI kinases networks

Pathway analysis was performed to determine if any biological processes were enriched in the networks (Figure 3A). All networks were enriched in processes involving the cytoskeleton, such as microtubule dynamics and neurite morphology, which is consistent with previous reports on these kinases in the brain [29, 30]. For instance, the beta isoform of CAMK2 can directly interact with F-actin to regulate synaptogenesis [31]. Protein translation and cell death were significantly enriched only in the ERK2 network. CAMK2A and ERK2 networks were also enriched in synaptic plasticity pathways, such as LTP (long-term potentiation), which is necessary for learning and memory. Akt3, ERK2, and CAMK2A are expressed in various cell types (i.e. neurons and glia) and subcellular compartments, including synapses[32]. Based on this enrichment in synaptic processes, the number of synaptic proteins in the networks was determined. Synaptic proteins were significantly enriched in all networks (Figures 3B, 3C, S3, and S4). The CAMK2A network contained the largest percentage of synaptic proteins with 67% and the Akt network had the least with 42%. This is consistent with previous studies demonstrating the regulation of synaptic plasticity by Akt, CAMK2, and ERK2. It has been demonstrated that ERK activation is necessary for LTP *in vivo* in the rodent hippocampus and required for different learning and memory laboratory paradigms [33]. A certain threshold of calcium can displace an inhibitory element on CAMK2 and this resulting calcium independence has been proposed to be the molecular mechanism necessary for synaptic plasticity and memory[34]. There is less direct evidence for Akt to be essential for synaptic plasticity consistent with the pathway analysis, but numerous reports have demonstrated a modulatory role [35]. The significant enrichment of synaptic proteins in the PPI networks generated from unfractionated hippocampi suggests the major role of these multifunctional kinases is regulation of synaptic plasticity.

PPI kinase networks associated with specific neurodevelopmental disorders

Since synaptic dysfunction is hypothesized to underlie numerous neurodevelopmental disorders (NDD), we examined if any of these kinase networks were enriched in genes implicated in autism spectrum disorder (ASD), fragile-X syndrome(FXS), schizophrenia (SCZ), and intellectual disability (ID) [36] [37] [38].

ID, former known as mental retardation, is characterized by deficits in intellectual and adaptive functioning. ASD is complex group of neurodevelopmental disorders characterized by deficits in social interaction, communication and repetitive stereotyped behaviors. SCZ is a complex neuropsychiatric disorder with symptoms including hallucinations, delusions, paranoia, disorganized thoughts, social isolation, and cognitive deficits. These disorders involve dysfunction in multiple brain regions including the hippocampus. Consistent with the heterogeneity of clinical phenotypes and the complexity of the genetics of these disorders, disease associated genetic variation (i.e. rare de novo mutations) has been detected in hundreds of genes in the human population. The enrichment of PPI network proteins associated with these diseases using recent DNA variant association studies was calculated[39–41]. All kinase networks were significantly enriched in proteins that have been associated with autism, only the Akt3 network was significantly enriched in SCZ associated genes and none of the networks were enriched with genes associated with ID

(Figure 4A and TableS4). FXS differs from the other NDD, because the genetic cause is known. A genetic mutation of the FMRP gene prevents the expression of the FMRP protein. How the FMRP mutation causes FXS is still unclear. FMRP is an RNA-binding protein that regulates translation. It has been postulated that the mRNAs that FMRP regulates could provide insight into FXS pathogenesis. For the FXS analysis, proteins whose mRNA binds FMRP was employed for the enrichment test [42]. All kinase networks were significantly enriched in proteins coded by mRNAs that bind FMRP (Figure 4A and TableS4). This is not the first report of ERK2, CAMK2A, and Akt being associated with these disorders. In the datasets used for the enrichment analysis, Akt3, CAMK2B, and CAMK2G were reported to be significantly associated with ASD and Akt3, CAMK2A, and CAMK2B were identified as targets of FMRP. Hyperactivation of ERK signaling has been reported in the brains of a mouse model of FXS and in the brains of FXS patients[43]. FMRP was also identified in our ERK2 network. Previous reports have suggested a role of the Akt signaling pathway in SCZ[44]. There is clinical overlap between ASD, FXS, ID, and SCZ. For example, FXS is the most common genetic cause of ID and is also associated with autistic phenotypes[45]. Accumulating evidence based on DNA variants in patients has revealed that there is also a molecular overlap, indicating a shared pathological mechanism [46]. Our data corroborates this idea, except for ID. This could suggest that our kinase signaling networks may underlie the shared autistic phenotype in these NDD, but the abnormality underlying the ID phenotype is dictated by different signaling systems not examined in this study. Importantly, our data demonstrates novel structural relationships between the proteins significantly associated with different NDD. This may explain how rare de novo mutations in different genes may result in similar clinical phenotypes by disrupting a common signaling PPI network.

Signaling complex prototype identified in the kinase PPI networks

Next, the kinase networks were queried for three protein functional groups previously reported to be involved in phosphorylation signaling: scaffolding proteins, kinases, and phosphatases. Annotating a protein definitively as a scaffold is elusive, as proteins with a variety of functions have been described as scaffolds in the literature. Two approaches were employed to identify all the known and potential novel scaffolding proteins in the networks. Since the defining characteristic of scaffolding proteins is the ability to bind multiple proteins simultaneously, the networks were analyzed with Scansite to identify protein binding motifs [47]. Half of the proteins in each network contained at least one binding domain (Figure 4B and TableS5). In all three networks, twenty-five unique proteins contained more than 5 binding domains which we classified as potential scaffolding proteins. Second, the annotations of the network proteins in the Uniprot knowledgebase[48] were searched for the terms “scaffolding” or “adaptor”. Twelve proteins were identified, and six of these proteins were also identified with Scansite to contain more than 5 protein binding domains. Two known PKA scaffolding proteins in the ERK2 network, AKAP5 and AKAP12, were not identified from our binding domain classification with each having one and two binding domains, respectively. Thus, using the number of binding domains solely to identify a scaffolding protein is not sufficient. On the other hand, some proteins that were identified with >5 protein binding domains are often described as scaffolding proteins in the literature but these descriptive terms were not used in the Uniprot annotations.

For example, PSD95(i.e. Dlg4) is a well-known scaffolding protein at the excitatory post-synaptic density but not annotated as one in Uniprot. In total, 31 proteins in the kinase networks were classified as scaffolding proteins using Uniprot and Scansite (Figure 4C), and they possess a variety of other protein functions. Iqsec3(IQ motif and SEC7 domain-containing protein 3) belongs to a family of ADP ribosylation factor-guanine nucleotide exchange factors and there is emerging evidence that this family comprises synaptic scaffolds[49]. The kinase MAST1 has previously been hypothesized to be a signaling scaffold due to its multiple binding domains[50]. Next, PPI networks were searched for phosphatases. Phosphatases are the enzymes that remove the phosphorylation moiety on the protein substrates. There are 5-fold fewer phosphatase genes than kinase genes, but they still play a vital role in kinase signaling specificity, and are also considered as promising drug targets[51]. Phosphatases were identified in all the kinase networks. Phosphatases from three structurally distinct protein families were identified: Phosphoprotein phosphatases (Ppp5c and Ppp3cb (aka. calcineurin)), Protein tyrosine phosphatases (Ptprn and Acp1), and protein phosphatase metal family(Ppm1e). Two phosphatases were identified in each of the kinase networks with Protein phosphatase 1E(Ppm1e) localized to both ERK2 and CAMK2A networks (Figure 4D). Ppm1e has previously been reported to dephosphorylate synaptic CAMK2[52]. Finally, the PPI networks were searched for kinases not in the gene family of the bait. Eleven and ten percent of the ERK2 and CAMK2 networks, respectively, were identified as protein kinases, while only seven percent of the Akt3 network was annotated as a kinase (Figure 4E). More than 50% of the kinases in the CAMK2A network were also in the ERK2 network, but there was no overlap between the CAMK2A and Akt3 networks. All kinase groups were represented except the TKL (tyrosine kinase-like group) and the smallest kinase group CK1(cell kinase 1). The AGC group was the most observed in the ERK2 and CAMK2A network, and tyrosine kinases in the Akt3 network. The most abundant gene family was the PKA gene family (i.e. PRKACA, PRKAR1A, PRKAR1B, PRKAR2A, and PRKAR2B), which was only identified in the ERK2 network. In addition, the documented PKA scaffolding proteins, AKAP5 and AKAP12, were only identified in the ERK2 network. This corroborates the previously reported functional cross-talk between the ERK and PKA signaling pathways, which critical for synaptic plasticity [53]. Classically, PKA has been demonstrated to phosphorylate the upstream regulator (i.e. Raf) of ERK2[54], but there are other functional intersection points of these pathways and some of these are also present in the ERK2 network. Rheb (identified in the ERK2 network) has been reported to regulate ERK2 activity through its interaction with Raf, and this interaction is regulated by PKA[55]. PKA is regulated by cAMP and regulation of cAMP by ERK2 serves as another intersection point. Phosphodiesterases (PDE) hydrolyze cAMP. ERK2 has been reported to bind and phosphorylate PDE4 isoforms and regulate their activity[56]. PDE10a was identified in the ERK2 network. Although this is the first report of ERK2 and PDE10a in a complex together, further insight into PDE10a biology is important, as drugs that regulate PDE10a have been proposed to treat a number of CNS disorders[57]. cAMP can also activate ERK2 independent of PKA activation through Rapgef2 or CNrasGEF, which was identified in the ERK2 network [58]. Overall, the well-studied cross-talk between the PKA and ERK pathways was represented in our ERK2 network indicating there is a structural component to the integration of these different kinase signaling pathways. Furthermore, this also suggests

that other non-bait kinases in the networks represent unexplored and complex communication between different kinase signaling pathways.

Identification of Potential Substrates

Due to the transient nature of the kinase-substrate interaction, it is not expected that the kinase-substrate interaction would be preserved using the techniques employed in this study[59]. Signaling complexes, however, have been postulated to facilitate phosphorylation by anchoring kinases and their substrates in the same vicinity. To identify potential substrates in these possible kinase-signal complexes, the Akt3 and ERK2 networks were searched for proteins containing the Akt (i.e. RXRXXS/T) or the ERK(i.e. PXS/TP) phospho-motif, respectively. About 30% of the network proteins contained the motif of the bait kinase, which included previously reported substrates (Figure 5A and B and TableS6 and S7). Next, it was tested whether the phospho-motifs were enriched in the appropriate network. The Akt and ERK motifs were observed in all kinase networks with no obvious differences (Figure 5C).

In addition, the frequency of these motifs was calculated for the whole rat proteome and the synaptic proteome. Interestingly, there was a greater percentage of both motifs in the synaptic proteome compared to the whole proteome and even larger increase motif frequency in the kinase networks compared to the whole proteome. Further analysis revealed that many of these proteins contained both an Akt motif and an ERK motif (Figure 5D). It is unclear if this lack of specificity is biological or an artifact. The tremendous amount of kinase cross-talk represented by the large variety of kinases in each of the networks may be preventing a definitive enrichment of substrates for one kinase. For instance, the transcription factor CREB (cAMP response element binding protein) has been reported to be phosphorylated at serine-133 by multiple kinase signaling pathways including Akt, CAMKIV, CAMKII, ERK, PKA, and PKC [60–63]. The increase frequency of motif containing proteins in our networks over the whole proteome also suggest an enrichment in potential substrates but the ability to selectively enrich for one kinase network may be impossible due to this cross-talk. Alternatively, it has been predicted that the number of residues that match a consensus phosphorylation motif in the entire proteome is well above the actual number of substrates[4]. This problem then is compounded by the fact that many kinases have identical or overlapping motifs. For example, the AKT consensus motif is RXRXXS/T, while CAMK2A is RXXS/T[4, 64]. Regardless, it was hypothesized that the existence of a kinase phospho-motif, combined with being designated as a highly confident member of that kinase's network, could suggest a potential functional relationship. The Akt or ERK2 phospho-motif containing proteins were examined for an unreported substrate with a known function that could be measured quantitatively to test this hypothesis. We chose to further investigate the cation channel HCN1 (Potassium/sodium hyperpolarization-activated cyclic nucleotide-gated channel 1) in the Akt3 network. HCN1 contains a Akt phosphorylation motif (i.e. $RMRTQS_{563}$) which is conserved in mouse and human sequences. First, we confirmed the interaction by immunoblot analysis (Figure 6A). HCN1 immunoreactivity was detected in the Akt IP but not in the ERK2 IP or control IP in the hippocampus. HCN1 was not detected in the starting IP material, indicating a considerable enrichment in the Akt IP. HCN1 was detected after the membranes were enriched but at a

lower molecular weight (MW) compared to the HCN1 immunoreactivity in the Akt IP. The high MW band could represent HCN1 in a homodimer complex or post-translational modified HCN1. This suggests that Akt may interact with a specific subset of the HCN1 pool in the hippocampus. Next, immunohistochemistry was performed in the hippocampus to determine if Akt and HCN1 are localized in similar subcellular compartments that would allow an interaction to occur *in vivo*. Intense HCN1 staining was observed in the distal dendrites of the CA1 region of the hippocampus, where HCN1 has previously been observed to be enriched by microscopy[65]. Akt was colocalized with HCN1 in these dendrites using the dendritic marker MAP2 (Figure 6B and FigureS5). Finally, the HCN1 mediated current (H-current, Ih) was measured in rat hippocampal slices with and without the Akt inhibitor, MK-2206. Recordings obtained from CA1 pyramidal neurons showed that MK-2206 significantly increased lh amplitude, indicating that Akt signaling negatively regulates HCN1 activity (Figure 6C and 6D).

It is important to note that while the recording conditions (voltage-protocol used to elicit Ih) and specific data analysis used here allows for the selective isolation of Ih, it does not rule out the possibility that other channels contribute to the effect of inhibition of Akt on Ih measured. Overall, the identification of a functional interaction between Akt and HCN1 suggests other phospho-motif containing network proteins may also be a resource for novel functional interaction.

HCN1 is a transmembrane protein that belongs to a family (i.e. HCN1–4) of channels. The active channels consist of homo- and hetero-tetramers which depolarize the membrane. We did also identify a previously reported binding partner of HCN1, Pex5l or Trip8b, which regulates the cell surface expression of HCN1 through binding to its C-terminal cytoplasmic tail [28]. The proposed Akt phosphorylation site and Pex5l interaction site are both on the C-terminal cytoplasmic tail, so it is tempting to speculate that Akt phosphorylation could affect HCN1 trafficking by regulating the HCN1/Pex5l interaction. Indeed, this possibility is consistent with our finding that inhibition of Akt increases Ih amplitude, which could be due to a change in open probability of the channel or increased surface expression. Akt has previously been demonstrated to regulate the trafficking of gamma-aminobutyric acid receptors to the plasma membrane to regulate synaptic strength[35]. Manipulation of other phosphorylation signaling pathways (i.e. calcineurin, PKC, p38MAPK, and PP1) have been reported to alter HCN activity[66, 67].

Both Akt and HCN1 have been reported to be involved in epilepsy, which encompasses a group of neurological disorders characterized by irregular neuronal discharges known as seizures. Epilepsy is the fourth most common neurological disorder. Multiple animal models of epilepsy have demonstrated a decreased HCN1 function upon the induction of seizures in the CA1 region of the hippocampus[68]. Acutely after seizure induction, HCN1 is internalized and removed from the dendritic membrane and more chronic timepoints have demonstrated a reduction in total HCN1 protein expression[69, 70]. Consequently, up-regulation of HCN activity returned neuronal excitability to control levels in a seizure animal model[67]. Furthermore, clinically used anti-epileptic drugs have been reported to modulate Ih[71, 72]. In human patients, Ih has been reported to be reduced in neurons[73]. In separate study, de novo mutations in HCN1 have been identified in patients with infantile

epileptic encephalopathy in a large exome sequencing study[74]. Similarly, many regulators of Akt and downstream targets of Akt have also been implicated in seizures and epilepsy in animal models [75]. An Akt mutant, which possesses increased kinase activity, has been identified in mice that displayed increased sensitivity for seizures in a phenotype-based chemical mutagenesis screen [76]. In humans, somatic mutations have been identified in Akt3 that suggest that stimulation of Akt may be involved in some forms of epilepsy[77–79]. Thus, down-regulation of HCN1 and activation of Akt are both associated with epilepsy, and we demonstrated that an Akt inhibitor can increase the activation of the HCN1. Further investigation into the ability of Akt to regulate HCN1 may provide a better molecular understanding of epilepsy.

Conclusions

In summary, we constructed a structural map of three distinct kinase signaling pathways crucial to hippocampal function, providing new molecular details of phosphorylation signaling in this complex tissue. With previously reported direct interactions of the kinases identified, we presume there are also novel direct interactions in this dataset. Due to the nature of the experimental design, additional experimentation is needed to determine if the proteins in the networks form a direct interaction with the bait kinase opposed to a functional interaction as reported for Akt and HCN1. We speculate that our kinase networks consist of multiple signaling complexes in different subcellular compartments as opposed to a single massive signaling complex. There was a significant enrichment of synaptic proteins in all the kinase networks, so the synapse is one subcellular compartment where some of these signaling complexes are localized. Although the kinases in this study were from evolutionally distinct gene families, there were four functional groups (i.e. scaffolding proteins, kinases, phosphatases and substrates) found in all the networks, identifying the common structural components of kinase signaling complexes *in vivo*. The proteins of each network, however, were unique. Our data also provides strong evidence for a structural component to the well-studied functional ERK-PKA cross-talk relationship and suggests structural cross-talk relationships is common within the kinome. Finally, these kinase PPI networks were enriched in proteins associated with ASD, signifying the importance of the data to spur additional studies for advancing translational research on this neurological disorder.

Materials and Methods

Animals for PPI experiments

A total of 18 male Sprague-Dawley rats (Harlan Laboratories, San Diego, CA), weighing 300 to 400 g, were used in these studies. Animals were housed in pairs in clear plastic cages located inside a temperature- and humidity-controlled animal colony and were maintained on a reversed day/night cycle (lights on from 7:00 P.M. to 7:00 A.M.). Food (Harlan Teklad, Madison, WI) and water and food ad libitum. Animal facilities were AAALAC-approved, and protocols were in accordance with the “Guiding Principles in the Care and Use of Animals” (provided by the American Physiological Society) and the guidelines of the National Institutes of Health. Rats were lightly anesthetized with isoflurane and sacrificed

by decapitation. Brains were removed and dissected, placed in dry ice-cooled isopentane for 5 sec, and stored at −80° C.

Immunoprecipitations

Each hippocampus was homogenized in 4mM HEPES, pH7, 200mM NaCl with protease and phosphatase inhibitors with an Eppendorf dounce grinder. Immunoprecipitation (IP) buffer(4mM HEPES, pH7, 200mM NaCl, 0.5% Triton, 0.5% NP-40, and 0.01% Sodium Deoyxcholate) was added to the homogenates and incubated overnight. The homogenates were centrifuged for 30min at 17,000 × g. The pellets were homogenized with IP buffer and incubated for 1hour. The homogenates were centrifuged for 30min at 17,000 × g. The two supernants were combined and a BCA protein assay(Fisher Scientific) was performed. Normal sera bound to Protein A(Life Technologies) or Protein G (Abcam) beads were added and incubate overnight. The precleared supernant was divided into two Eppendorf tubes and either beads cross-linked to the bait kinase antibody(anti-Akt rabbit Abcam #ab6076, anti-ERK2 rabbit scbt# sc-154, and anti-CAMK2 mouse abcam# Ab22609) or beads cross-linked to the normal sera were added. Mouse antibodies were crosslinked to Protein G beads and rabbit antibodies were crosslinked to Protein A beads. The beads were incubated with supernants overnight and then washed three times. The beads were frozen at −80C until protein digestion. IP for immunoblots were prepared identically except antibodies were not crosslink to the beads. After antibody incubation with the precleared supernant, beads were added and incubated overnight.

Protein Digestion

Proteins were eluted twice from the beads with 5% SDS, then boiled for 10min. The elution was precipitated with methanol and chloroform. The precipitate was digested with ProteaseMAX(Promega) as previously described[80].

Mass Spectrometry Analysis

Each digestion was analyzed twice by MS analysis for two technical replicates per IP. For each technical replicate, 15ul of the digestion was injected directly onto a 50cm 100um i.d. capillary containing 1.7μm BEH C18 resin (Waters). Peptides were separated at flow rate of 300nl/min on Easy-nLC 1000 (Thermo) on 220min reverse-phase gradient. Peptides were eluted from the tip of the column and nanosprayed directly into an Elite mass spectrometer(Thermo) by application of 2.5kV voltage at the back of the column. The Elite was operated in a data dependent mode. Full MS1 scans were collected in the orbitrap at 240K resolution and 20 rapid CID MS/MS in the ion trap[81]. Dynamic exclusion was used with exclusion duration of 30 sec.

Interpretation of Tandem Mass spectra

Data from technical replicates were combined prior to database searching. MS2 (tandem mass spectra) were extracted from the XCalibur data system format (.RAW) into MS2 format using RawConverter[82]. The MS2 files were interpreted by Prolucid and results were filtered, sorted, and displayed using the DTA Select 2 program using a decoy database strategy filtering with a 5ppm mass accuracy [83, 84]. Searches were performed against

UniProt_rat_reviewed_iso_cont_03-25-2014. For each MS dataset (i.e. two technical replicates), the protein false discovery rate was < 1%.

Bioinformatic Analyses

The options for SAINT analysis were low mode option off, minfold option on, normalization by spectral count off, normalization by length off, burn time of 5000 and main iterations of 20000. The SAINT analysis was run with all bait and control identifications in one analysis. The pathway enrichment analysis (Figure 3A) was performed with the software, Ingenuity, which also generated the heat map[85]. For enrichment analysis of disease associated genes(Figure 4A), our networks were compared to four published list of genes associated to a neurodevelopmental disorder: autism spectrum disorder (ASD)[39], fragile-X syndrome(FXS)[42], schizophrenia (SCZ)[40], and intellectual disability (ID)[41]. For the SCZ list, the silent genes were removed. To calculate the enrichment significance of synaptic proteins in the kinase networks(Figure 3B), proteins identified from a published MS analysis of synapses was used[32]. This synaptic dataset was also used for Figure 5C and 5D for the "synaptic proteome" analysis. The rat Uniprot database used for MS identifications was also used for the "whole proteome" analysis in Figure 5C and 5D. For all enrichment tests, one-tailed Fisher's Exact test was performed using a two-sided alpha level of 0.05 to determine if there was significant enrichment over background as previously described[86]. The background dataset was all the expressed mRNAs in purified mouse cortical neurons as reported by Zhang et al[87]. To identify protein binding motifs (Figure 4C), protein sequences were analyzed by Scansite using the highest stringency setting. For STRING analysis (Figure 2C–E), functional interactions were only counted if there was "experimental evidence" with medium confidence in the STRING database.

Immunohistochemistry

Three two-month-old Sprague-Dawley rats were deeply anesthetized with halothane and transcardially perfused with ~150 mL of PBS and then with ~200 mL of 4% paraformaldehyde in PBS (15 mL/min). The brains were removed and placed in the fixative at 4°C o/n for the post-fixation and cryoprotected in 30 % sucrose in PBS for two days and then for another day in a new 30% sucrose in PBS. Frozen brains were sectioned into 40 μm-thick slices using a cryostat. For immunofluorescence staining, the brain slices were washed with PBS and then incubated in 1× citrate buffer pH 6.0 (Thermo Scientific) at ~95°C for 10 min. After 3 times of washing in PBS-T (PBS with 0.5 % Triton X-100), slices were incubated in blocking solution (5% donkey serum, 0.5% Triton X-100 in PBS) for 1 h at RT and then with primary antibodies at 4°C overnight (guinea pig anti-HCN1 1:100 (Alomone #AGP-203), rabbit anti-AKT 1:50 (Cell Signaling #9272), chicken anti-MAP2 1:1000 (Abcam #ab5392)). After 3 times of washing in PBS-T, slices were incubated with secondary antibodies at RT for 2 h (1:100, Alexa Fluor 488-AffiniPure donkey anti-guinea pig IgG, Alexa Fluor 594-AffiniPure donkey anti-rabbit IgG, DyLight 405-AffiniPure donkey anti-chicken IgY) and then washed with PBS-T 3 times. ProLong Diamond was used for mounting the brain slices on the slide glass. Fluorescence was detected by confocal microscopy (LSM710). Control groups omitting either AKT or HCN1 antibody were processed simultaneously and imaged with the same condition (Supplementary Figure 1). Figure 6B is a representative image from the analysis of three rats.

Hippocampal Slice Preparation

Six male Sprague Dawley rats (80–150g) were used for electrophysiological recordings. Rats were briefly anesthetized with 3–5% isoflurane and decapitated. Brains were quickly dissected out and coronal hippocampal slices (300μm) were sectioned using a vibratome (Leica 1000S, Leica Biosystems) in ice cold cutting solution containing (in mM): 125 NaCl, 2.5 KCl, 1.25 NaHCO3, 4 MgCl2, 10 D-glucose, 15 sucrose, 0.4 ascorbic acid, pH 7.3. Slices were then incubated at 32°C for 30mins in the oxygenated (95% O2/5% CO2) cutting solution also containing 2mM kynurenic acid to protect against excitotoxicity. Subsequently, slices were transferred into ACSF containing (in mM): 130 NaCl, 3.5 KCl, 1.25 NaH2PO4, 1.5 MgSO4, 2 CaCl2, 24 NaHCO3, 10 D-glucose, pH 7.3 for a minimum of 30mins at room temperature prior to recording.

Electrophysiological Recordings

Patch pipettes were fabricated from borosilicate glass (Warner Instruments) to a resistance of 2–4MΩ with a vertical puller (PC-10, Narishige) and filled with an intracellular solution containing (in mM): 145 K-gluconate, 0.5 EGTA, 2 MgCl2, 10 Hepes, 2 Na-ATP, 0.2 Na-GTP, pH 7.2. Cells were visualized with infrared differential interference contrast (IR-DIC) optics under a 60× water immersion objective using a CCD camera (Infinity 3s, Lumenera). Pyramidal neurons (>80pF capacitance) in the CA1 region were targeted for recordings. Whole-cell patch clamp recordings were obtained with a sampling rate of 20kHz and filtered at 10kHz using Multiclamp 700B amplifier, DigiData 1550B and pClamp 10 software (Molecular Devices, Sunnyvale, CA). Series resistance was not compensated but monitored throughout the experiment, and cells with a series resistance >15MΩ or a >20% change were excluded. Cells were clamped at −70mV. To assess Ih, current-voltage curves were generated using a voltage protocol consisting of 1 sec hyperpolarizing steps ranging from −60mV to −120mV (15mV increment) from a holding potential of −50mV. We quantified Ih as the difference between the current of the relaxation at the peak observed at the onset of the hyperpolarizing voltage step (following the capacitance artifact) and the current measured just before the end of the voltage step. Drug effects were assessed after 12mins of superfusion of the drug in ACSF. Data points represent the mean ± SEM and statistical analysis was assessed with a two-way ANOVA using Prism 6 (Graphpad Prism).

Immunoblot Analysis

After the IP, the beads were resuspended using 4× Laemmli Sample Buffer (Bio-Rad). For membrane enriched sample (i.e. Input2 Figure 6A), one hippocampus was homogenized in 4mM HEPES pH 7.0, 200mM NaCl. Membranes were pelleted by centrifugation at 21,000 × g for 10min. The membrane pellet was washed with homogenization buffer and then pelleted again. The membrane pellet was resuspended with IP buffer. After centrifugation at 21,000 × g for 10min, the supernant was used as the membrane enriched sample. Samples were separated with 4–12% Bis-Tris gradient gel(Life Technologies), transferred to PVDF blotting paper, and developed as previously described[88]. The immunoblotting antibodies were mouse HCN1 (UC Davis/NIH NeuroMab Facility, clone N70/28), anti-ERK2(mouse scbt #sc-1647), and anti-Akt (mouse scbt #sc-5298). The immunoblot analysis was performed in four different rats with Akt and HCN1 and Figure 4E is a representative image.

Supplementary Material

Refer to Web version on PubMed Central for supplementary material.

Acknowledgements

We thank Dr. Paul Schweitzer(TSRI)for his expert advice on HCN1 electrophysiology, Tobias Ehrenberger (MIT) for performing the ScanSite analyses, and Dr. Claire Delahunty(TSRI) for critical review of the manuscript.

Funding

This work has been supported by NIH grants P41 GM103533, R01 MH067880 (to J.R.Y.) and AA015566 (to M.R.). MLA holds a Discovery Grant from the Natural Sciences and Engineering Research Council of Canada (NSERC) and startup funds from the University of Ottawa.

References

1. Manning G, et al., The protein kinase complement of the human genome. Science, 2002 298(5600): p. 1912–34. [PubMed: 12471243]
2. Alexander J, et al., Spatial exclusivity combined with positive and negative selection of phosphorylation motifs is the basis for context-dependent mitotic signaling. Sci Signal, 2011 4(179): p. ra42. [PubMed: 21712545]
3. Duarte ML, et al., Protein folding creates structure-based, noncontiguous consensus phosphorylation motifs recognized by kinases. Sci Signal, 2014 7(350): p. ra105.
4. Manning BD and Cantley LC, AKT/PKB signaling: navigating downstream. Cell, 2007 129(7): p. 1261–74. [PubMed: 17604717]
5. Berndt N, Karim RM, and Schonbrunn E, Advances of small molecule targeting of kinases. Curr Opin Chem Biol, 2017 39: p. 126–132. [PubMed: 28732278]
6. Herskowitz I, MAP kinase pathways in yeast: for mating and more. Cell, 1995 80(2): p. 187–97. [PubMed: 7834739]
7. Sanderson JL and Dell'Acqua ML, AKAP signaling complexes in regulation of excitatory synaptic plasticity. Neuroscientist, 2011 17(3): p. 321–36. [PubMed: 21498812]
8. Schechtman D and Mochly-Rosen D, Isozyme-specific inhibitors and activators of protein kinase C. Methods Enzymol, 2002 345: p. 470–89. [PubMed: 11665630]
9. Yarwood SJ, et al., The RACK1 signaling scaffold protein selectively interacts with the cAMP-specific phosphodiesterase PDE4D5 isoform. J Biol Chem, 1999 274(21): p. 14909–17. [PubMed: 10329691]
10. Chang BY, et al., RACK1, a receptor for activated C kinase and a homolog of the beta subunit of G proteins, inhibits activity of src tyrosine kinases and growth of NIH 3T3 cells. Mol Cell Biol, 1998 18(6): p. 3245–56. [PubMed: 9584165]
11. Park SH, Zarrinpar A, and Lim WA, Rewiring MAP kinase pathways using alternative scaffold assembly mechanisms. Science, 2003 299(5609): p. 1061–4. [PubMed: 12511654]
12. Huttlin EL, et al., A tissue-specific atlas of mouse protein phosphorylation and expression. Cell, 2010 143(7): p. 1174–89. [PubMed: 21183079]
13. Trinidad JC, et al., Quantitative analysis of synaptic phosphorylation and protein expression. Mol Cell Proteomics, 2008 7(4): p. 684–96. [PubMed: 18056256]
14. Ehlers MD, Reinsertion or degradation of AMPA receptors determined by activity-dependent endocytic sorting. Neuron, 2000 28(2): p. 511–25. [PubMed: 11144360]
15. Mufson EJ, et al., Molecular and cellular pathophysiology of preclinical Alzheimer's disease. Behav Brain Res, 2016 311: p. 54–69. [PubMed: 27185734]
16. Rigaut G, et al., A generic protein purification method for protein complex characterization and proteome exploration. Nat Biotechnol, 1999 17(10): p. 1030–2. [PubMed: 10504710]
17. Mohammed H and Carroll JS, Approaches for assessing and discovering protein interactions in cancer. Mol Cancer Res, 2013 11(11): p. 1295–302. [PubMed: 24072816]

18. Easton RM, et al., Role for Akt3/protein kinase Bgamma in attainment of normal brain size. Mol Cell Biol, 2005 25(5): p. 1869–78. [PubMed: 15713641]
19. Liu H, Sadygov RG, and Yates JR 3rd, A model for random sampling and estimation of relative protein abundance in shotgun proteomics. Anal Chem, 2004 76(14): p. 4193–201. [PubMed: 15253663]
20. Chao LH, et al., A mechanism for tunable autoinhibition in the structure of a human Ca2+/calmodulin- dependent kinase II holoenzyme. Cell, 2011 146(5): p. 732–45. [PubMed: 21884935]
21. Erondu NE and Kennedy MB, Regional distribution of type II Ca2+/calmodulin-dependent protein kinase in rat brain. J Neurosci, 1985 5(12): p. 3270–7. [PubMed: 4078628]
22. Mellacheruvu D, et al., The CRAPome: a contaminant repository for affinity purification-mass spectrometry data. Nat Methods, 2013 10(8): p. 730–6. [PubMed: 23921808]
23. Choi H, et al., SAINT: probabilistic scoring of affinity purification-mass spectrometry data. Nat Methods, 2011 8(1): p. 70–3. [PubMed: 21131968]
24. Orchard S, et al., The MIntAct project--IntAct as a common curation platform for 11 molecular interaction databases. Nucleic Acids Res, 2014 42(Database issue): p. D358–63. [PubMed: 24234451]
25. Fernandez E, et al., Targeted tandem affinity purification of PSD-95 recovers core postsynaptic complexes and schizophrenia susceptibility proteins. Mol Syst Biol, 2009 5: p. 269. [PubMed: 19455133]
26. Bingol B, et al., Autophosphorylated CaMKIIalpha acts as a scaffold to recruit proteasomes to dendritic spines. Cell, 2010 140(4): p. 567–78. [PubMed: 20178748]
27. Szklarczyk D, et al., STRING v10: protein-protein interaction networks, integrated over the tree of life. Nucleic Acids Res, 2015 43(Database issue): p. D447–52. [PubMed: 25352553]
28. Santoro B, et al., TRIP8b splice variants form a family of auxiliary subunits that regulate gating and trafficking of HCN channels in the brain. Neuron, 2009 62(6): p. 802–13. [PubMed: 19555649]
29. Earnest S, et al., Phosphorylation of dynamin by ERK2 inhibits the dynamin-microtubule interaction. FEBS Lett, 1996 396(1): p. 62–6. [PubMed: 8906867]
30. Nakai T, et al., Girdin phosphorylation is crucial for synaptic plasticity and memory: a potential role in the interaction of BDNF/TrkB/Akt signaling with NMDA receptor. J Neurosci, 2014 34(45): p. 14995–5008. [PubMed: 25378165]
31. Fink CC, et al., Selective regulation of neurite extension and synapse formation by the beta but not the alpha isoform of CaMKII. Neuron, 2003 39(2): p. 283–97. [PubMed: 12873385]
32. Collins MO, et al., Molecular characterization and comparison of the components and multiprotein complexes in the postsynaptic proteome. J Neurochem, 2006 97 Suppl 1: p. 16–23. [PubMed: 16635246]
33. Atkins CM, et al., The MAPK cascade is required for mammalian associative learning. Nat Neurosci, 1998 1(7): p. 602–9. [PubMed: 10196568]
34. Bear MF and Malenka RC, Synaptic plasticity: LTP and LTD. Curr Opin Neurobiol, 1994 4(3): p. 389–99. [PubMed: 7919934]
35. Wang Q, et al., Control of synaptic strength, a novel function of Akt. Neuron, 2003 38(6): p. 915–28. [PubMed: 12818177]
36. Bourgeron T, From the genetic architecture to synaptic plasticity in autism spectrum disorder. Nat Rev Neurosci, 2015 16(9): p. 551–63. [PubMed: 26289574]
37. Pfeiffer BE and Huber KM, Fragile X mental retardation protein induces synapse loss through acute postsynaptic translational regulation. J Neurosci, 2007 27(12): p. 3120–30. [PubMed: 17376973]
38. Pocklington AJ, O'Donovan M, and Owen MJ, The synapse in schizophrenia. Eur J Neurosci, 2014 39(7): p. 1059–67. [PubMed: 24712986]
39. Uddin M, et al., Brain-expressed exons under purifying selection are enriched for de novo mutations in autism spectrum disorder. Nat Genet, 2014 46(7): p. 742–7. [PubMed: 24859339]
40. Fromer M, et al., De novo mutations in schizophrenia implicate synaptic networks. Nature, 2014 506(7487): p. 179–84. [PubMed: 24463507]

41. Lelieveld SH, et al., Meta-analysis of 2,104 trios provides support for 10 new genes for intellectual disability. Nat Neurosci, 2016 19(9): p. 1194–6. [PubMed: 27479843]
42. Darnell JC, et al., FMRP stalls ribosomal translocation on mRNAs linked to synaptic function and autism. Cell, 2011 146(2): p. 247–61. [PubMed: 21784246]
43. Gantois I, et al., Metformin ameliorates core deficits in a mouse model of fragile X syndrome. Nat Med, 2017 23(6): p. 674–677. [PubMed: 28504725]
44. McGuire JL, et al., Abnormalities of signal transduction networks in chronic schizophrenia. NPJ Schizophr, 2017 3(1): p. 30. [PubMed: 28900113]
45. Hernandez RN, et al., Autism spectrum disorder in fragile X syndrome: a longitudinal evaluation. Am J Med Genet A, 2009 149A(6): p. 1125–37. [PubMed: 19441123]
46. Burbach JP and van der Zwaag B, Contact in the genetics of autism and schizophrenia. Trends Neurosci, 2009 32(2): p. 69–72. [PubMed: 19135727]
47. Ehrenberger T, Cantley LC, and Yaffe MB, Computational prediction of protein-protein interactions. Methods Mol Biol, 2015 1278: p. 57–75. [PubMed: 25859943]
48. The UniProt C, UniProt: the universal protein knowledgebase. Nucleic Acids Res, 2017 45(D1): p. D158–D169. [PubMed: 27899622]
49. Um JW, Synaptic functions of the IQSEC family of ADP-ribosylation factor guanine nucleotide exchange factors. Neurosci Res, 2017 116: p. 54–59. [PubMed: 27369185]
50. Lumeng C, et al., Interactions between beta 2-syntrophin and a family of microtubule-associated serine/threonine kinases. Nat Neurosci, 1999 2(7): p. 611–7. [PubMed: 10404183]
51. De Munter S, Kohn M, and Bollen M, Challenges and opportunities in the development of protein phosphatase-directed therapeutics. ACS Chem Biol, 2013 8(1): p. 36–45. [PubMed: 23214403]
52. Kitani T, et al., Post-translational excision of the carboxyl-terminal segment of CaM kinase phosphatase N and its cytosolic occurrence in the brain. J Neurochem, 2006 96(2): p. 374–84. [PubMed: 16269004]
53. Waltereit R and Weller M, Signaling from cAMP/PKA to MAPK and synaptic plasticity. Mol Neurobiol, 2003 27(1): p. 99–106. [PubMed: 12668903]
54. Dumaz N and Marais R, Protein kinase A blocks Raf-1 activity by stimulating 14-3-3 binding and blocking Raf-1 interaction with Ras. J Biol Chem, 2003 278(32): p. 29819–23. [PubMed: 12801936]
55. Karbowniczek M, Robertson GP, and Henske EP, Rheb inhibits C-raf activity and B-raf/C-raf heterodimerization. J Biol Chem, 2006 281(35): p. 25447–56. [PubMed: 16803888]
56. Baillie GS, et al., Sub-family selective actions in the ability of Erk2 MAP kinase to phosphorylate and regulate the activity of PDE4 cyclic AMP-specific phosphodiesterases. Br J Pharmacol, 2000 131(4): p. 811–9. [PubMed: 11030732]
57. Wilson LS and Brandon NJ, Emerging biology of PDE10A. Curr Pharm Des, 2015 21(3): p. 378–88. [PubMed: 25159072]
58. Li Y, et al., Protein Kinase A-independent Ras Protein Activation Cooperates with Rap1 Protein to Mediate Activation of the Extracellular Signal-regulated Kinases (ERK) by cAMP. J Biol Chem, 2016 291(41): p. 21584–21595. [PubMed: 27531745]
59. de Oliveira PS, et al., Revisiting protein kinase-substrate interactions: Toward therapeutic development. Sci Signal, 2016 9(420): p. re3.
60. Ho N, et al., Impaired synaptic plasticity and cAMP response element-binding protein activation in Ca2+/calmodulin-dependent protein kinase type IV/Gr-deficient mice. J Neurosci, 2000 20(17): p. 6459–72. [PubMed: 10964952]
61. Impey S, et al., Cross talk between ERK and PKA is required for Ca2+ stimulation of CREB-dependent transcription and ERK nuclear translocation. Neuron, 1998 21(4): p. 869–83. [PubMed: 9808472]
62. Socodato R, et al., The nitric oxide-cGKII system relays death and survival signals during embryonic retinal development via AKT-induced CREB1 activation. Cell Death Differ, 2014 21(6): p. 915–28. [PubMed: 24531539]

63. Mao LM, Tang Q, and Wang JQ, Protein kinase C-regulated cAMP response element-binding protein phosphorylation in cultured rat striatal neurons. Brain Res Bull, 2007 72(4–6): p. 302–8. [PubMed: 17452290]
64. Chen HJ, et al., A synaptic Ras-GTPase activating protein (p135 SynGAP) inhibited by CaM kinase II. Neuron, 1998 20(5): p. 895–904. [PubMed: 9620694]
65. Lorincz A, et al., Polarized and compartment-dependent distribution of HCN1 in pyramidal cell dendrites. Nat Neurosci, 2002 5(11): p. 1185–93. [PubMed: 12389030]
66. Williams AD, Jung S, and Poolos NP, Protein kinase C bidirectionally modulates Ih and hyperpolarization-activated cyclic nucleotide-gated (HCN) channel surface expression in hippocampal pyramidal neurons. J Physiol, 2015 593(13): p. 2779–92. [PubMed: 25820761]
67. Jung S, et al., Downregulation of dendritic HCN channel gating in epilepsy is mediated by altered phosphorylation signaling. J Neurosci, 2010 30(19): p. 6678–88. [PubMed: 20463230]
68. Brennan GP, Baram TZ, and Poolos NP, Hyperpolarization-Activated Cyclic Nucleotide-Gated (HCN) Channels in Epilepsy. Cold Spring Harb Perspect Med, 2016 6(3): p. a022384. [PubMed: 26931806]
69. Jung S, et al., Rapid loss of dendritic HCN channel expression in hippocampal pyramidal neurons following status epilepticus. J Neurosci, 2011 31(40): p. 14291–5. [PubMed: 21976514]
70. McClelland S, et al., Neuron-restrictive silencer factor-mediated hyperpolarization-activated cyclic nucleotide gated channelopathy in experimental temporal lobe epilepsy. Ann Neurol, 2011 70(3): p. 454–64. [PubMed: 21905079]
71. Poolos NP, Migliore M, and Johnston D, Pharmacological upregulation of h-channels reduces the excitability of pyramidal neuron dendrites. Nat Neurosci, 2002 5(8): p. 767–74. [PubMed: 12118259]
72. Peng BW, et al., Increased basal synaptic inhibition of hippocampal area CA1 pyramidal neurons by an antiepileptic drug that enhances I(H). Neuropsychopharmacology, 2010 35(2): p. 464–72. [PubMed: 19776733]
73. Wierschke S, et al., Hyperpolarization-activated cation currents in human epileptogenic neocortex. Epilepsia, 2010 51(3): p. 404–14. [PubMed: 19694789]
74. Nava C, et al., De novo mutations in HCN1 cause early infantile epileptic encephalopathy. Nat Genet, 2014 46(6): p. 640–5. [PubMed: 24747641]
75. Zeng LH, Rensing NR, and Wong M, Developing Antiepileptogenic Drugs for Acquired Epilepsy: Targeting the Mammalian Target of Rapamycin (mTOR) Pathway. Mol Cell Pharmacol, 2009 1(3): p. 124–129. [PubMed: 20419051]
76. Tokuda S, et al., A novel Akt3 mutation associated with enhanced kinase activity and seizure susceptibility in mice. Hum Mol Genet, 2011 20(5): p. 988–99. [PubMed: 21159799]
77. Baek ST, et al., An AKT3-FOXG1-reelin network underlies defective migration in human focal malformations of cortical development. Nat Med, 2015 21(12): p. 1445–54. [PubMed: 26523971]
78. Poduri A, et al., Somatic activation of AKT3 causes hemispheric developmental brain malformations. Neuron, 2012 74(1): p. 41–8. [PubMed: 22500628]
79. Lee JH, et al., De novo somatic mutations in components of the PI3K-AKT3-mTOR pathway cause hemimegalencephaly. Nat Genet, 2012 44(8): p. 941–5. [PubMed: 22729223]
80. McClatchy DB, et al., Global quantitative analysis of phosphorylation underlying phencyclidine signaling and sensorimotor gating in the prefrontal cortex. Mol Psychiatry, 2016 21(2): p. 205–15. [PubMed: 25869802]
81. Michalski A, et al., Ultra high resolution linear ion trap Orbitrap mass spectrometer (Orbitrap Elite) facilitates top down LC MS/MS and versatile peptide fragmentation modes. Mol Cell Proteomics, 2012 11(3): p. O111 013698.
82. He L, et al., Extracting Accurate Precursor Information for Tandem Mass Spectra by RawConverter. Anal Chem, 2015 87(22): p. 11361–7. [PubMed: 26499134]
83. Xu T, et al., ProLuCID: An improved SEQUEST-like algorithm with enhanced sensitivity and specificity. J Proteomics, 2015 129: p. 16–24. [PubMed: 26171723]
84. Lavallee-Adam M, et al., From raw data to biological discoveries: a computational analysis pipeline for mass spectrometry-based proteomics. J Am Soc Mass Spectrom, 2015 26(11): p. 1820–6. [PubMed: 26002791]

85. Calvano SE, et al., A network-based analysis of systemic inflammation in humans. Nature, 2005 437(7061): p. 1032–7. [PubMed: 16136080]

86. Wilkinson B, Li J, and Coba MP, Synaptic GAP and GEF Complexes Cluster Proteins Essential for GTP Signaling. Sci Rep, 2017 7(1): p. 5272. [PubMed: 28706196]

87. Zhang Y, et al., An RNA-sequencing transcriptome and splicing database of glia, neurons, and vascular cells of the cerebral cortex. J Neurosci, 2014 34(36): p. 11929–47. [PubMed: 25186741]

88. McClatchy DB, et al., Quantification of the synaptosomal proteome of the rat cerebellum during post-natal development. Genome Res, 2007 17(9): p. 1378–88. [PubMed: 17675365]

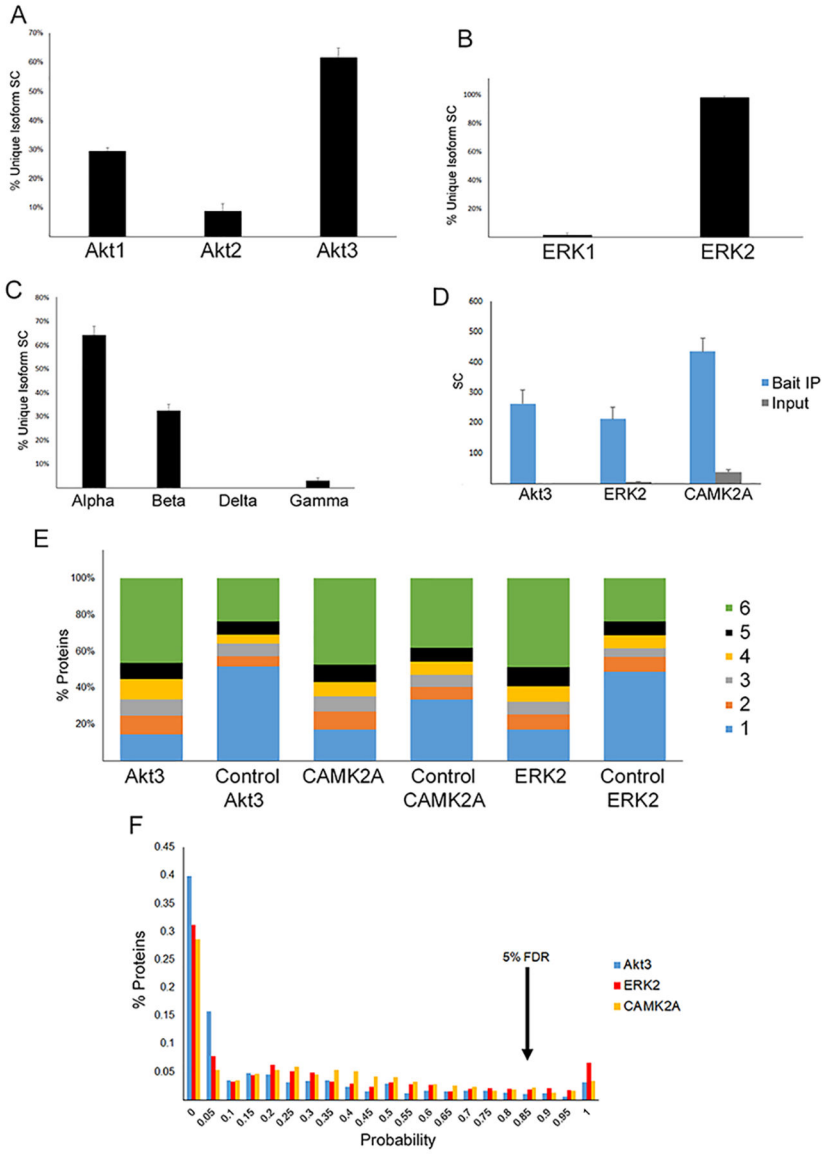

Figure 1.

The construction of kinase hippocampal PPI networks. **A**, Akt3 was the most abundant Akt isoform identified in the Akt IP-MS dataset. **B**, ERK2 was the most abundant ERK isoform identified in the ERK IP-MS dataset. **C**, CAMK2A was the most abundant CAMK2 isoform identified in the CAMK2 IP-MS dataset. For A-C, the spectra count(SC) for identified peptides that were unique to a kinase isoform was summed, then the percentage of SC for each isoform (y-axis) was calculated. The bar graph represents average percentage and standard deviation for six IP-MS analyses. **D**, The kinase baits are enriched in the IP-MS datasets. The average SC and standard deviation for kinase baits was calculated from six MS analyses of the bait IPs and six MS analyses of input (i.e. hippocampal lysates). **E**, Protein identifications are more reproducible in baits IPs than in control IPs. The colors represent the number of biological replicates that a protein was identified in. The y-axis is the percentage of proteins in an IP-MS dataset. **F**, Five percent FDR filter generates kinase PPI

network consisting of interactions with 85% probability or greater of being true. The histogram shows the probabilities assigned to every protein identified in the IP-MS datasets.

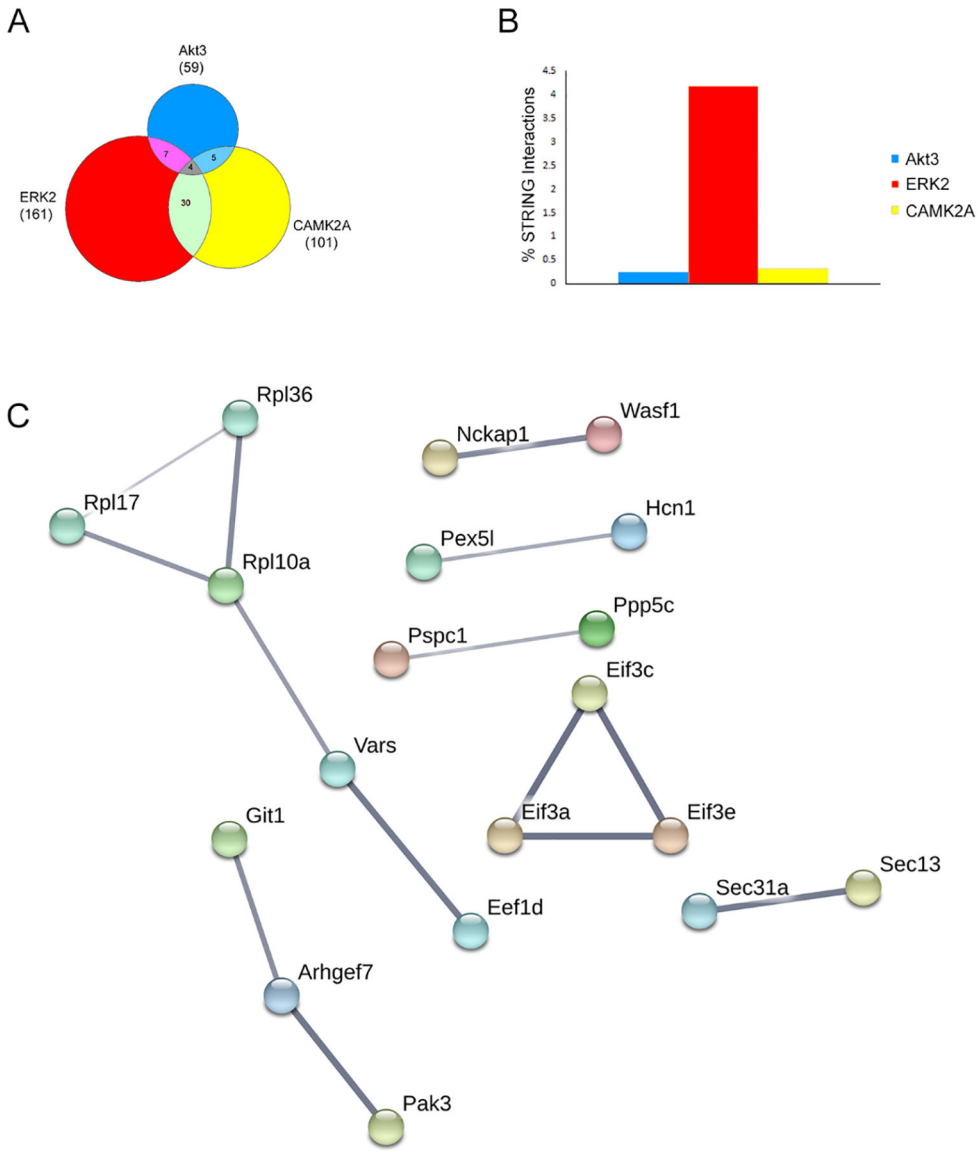

Figure 2.

A, Venn diagram of the proteins identified in kinase PPI networks. **B**, The percentage of binary STRING interactions identified in kinase PPI network normalized by the number of proteins in each network. **C**, Interactions between proteins within the Akt3 network annotated with the STRING database. Bait kinase isoforms (e.g. Akt1) were removed from all analyses.

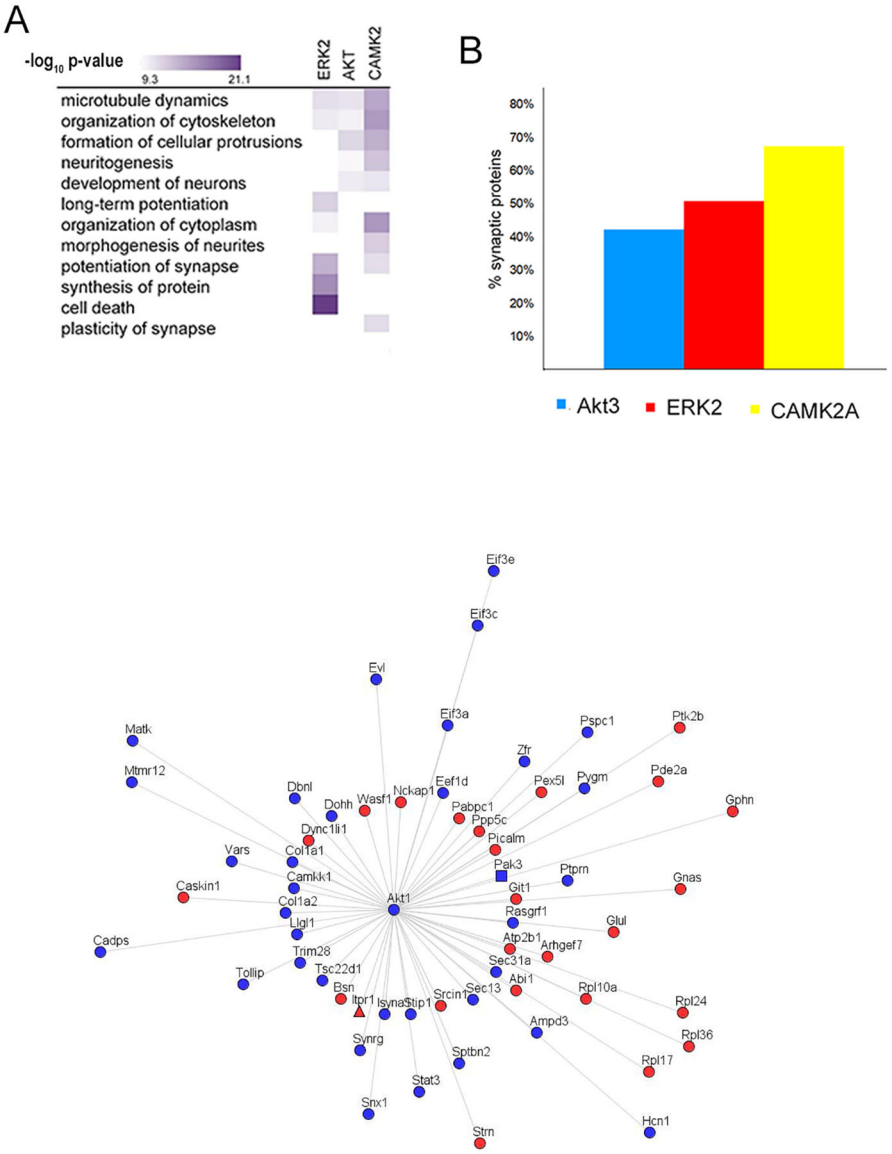

Figure 3.

A, Comparison of the biological processes significantly enriched in the kinase networks. The dark color represents a smaller p-value. **B**, The percentage of synaptic proteins in each of the kinase PPI networks. **C**, All proteins in the Akt3 network with the red circles indicating the synaptic proteins. The triangles represent proteins that have previously been reported to bind the bait kinase and the squares represent proteins that have isoforms that have previously been reported to bind the bait kinase. The distance from the center represents the approximate probability score with the closest to the center having the highest probability of being a true interactor. The gene names are directly above the symbols.

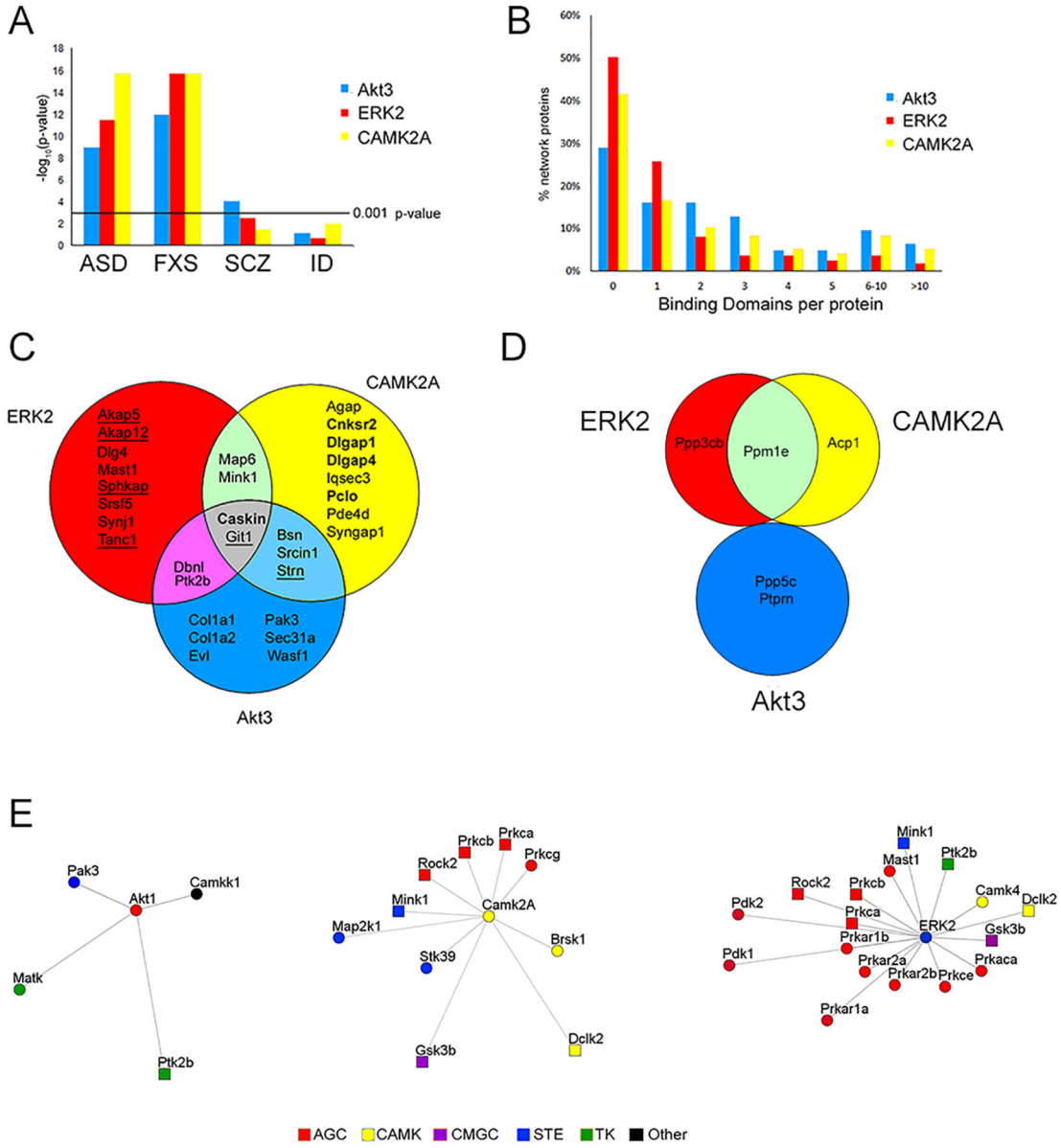

Figure 4.

A, Enrichment analysis of genes previously reported to be associated with different neurodevelopment disorders: autism spectrum disorder (ASD), Fragile-X syndrome(FXS), schizophrenia (SCZ), and intellectual disability (ID). The y-axis is the -log10 of the p-value with a p-value < 0.001 as the significance filter. **B**, Identification of potential scaffolding proteins in the kinase networks. The x-axis is the number of binding motifs identified in a protein and the y-axis is the percentage of proteins for each kinase network. **C**, A Venn diagram of the proteins with more than 5 binding motifs and proteins annotated as scaffolding or adaptor protein in Uniprot in the kinase networks. The gene names that are underlined were described as a scaffolding or adapter protein in their Uniprot description while gene names in bold were identified as scaffolding proteins with both Uniprot and Scansite.**D**, Venn diagram of phosphatases in the kinase PPI networks. **E**, Non-bait kinases

identified in the PPI networks. The color represents the kinase group. The square network nodes indicate kinases that were in two networks. The distance from the centered

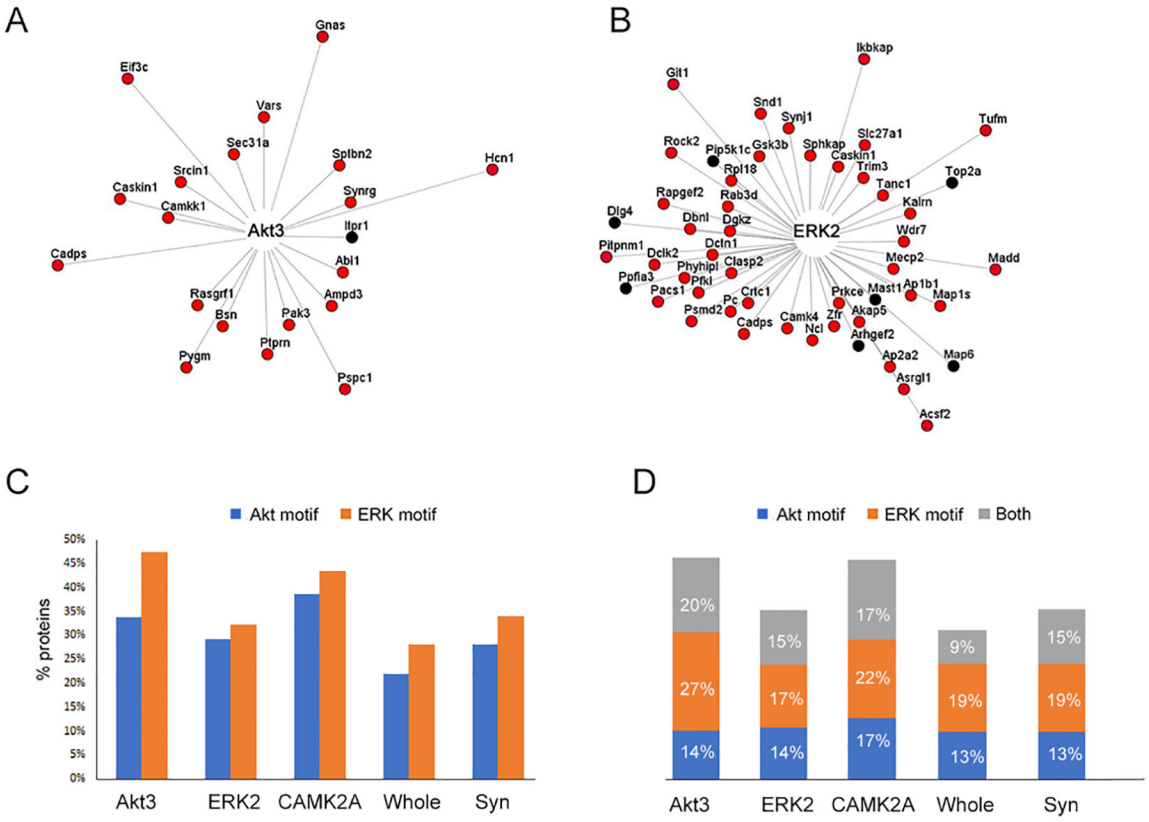

Figure 5.

Proteins containing an Akt motif in the Akt3 network (**A**) and ERK motif in the ERK2 network (**B**). Black circles represent previously reported substrates of the bait kinase. The distance from the centered bait kinase represents the approximate probability score with the closest to the center having the highest probability of being a true interactor. The gene names are directly above the symbols. **C**, The percentage of proteins in each kinase networks containing either an Akt motif or an ERK motif. **D**, The percentage of proteins containing an Akt motif, an ERK motif or both in the kinase networks. “Whole” represents the whole rat proteome and “Syn” represents the synaptic proteome.

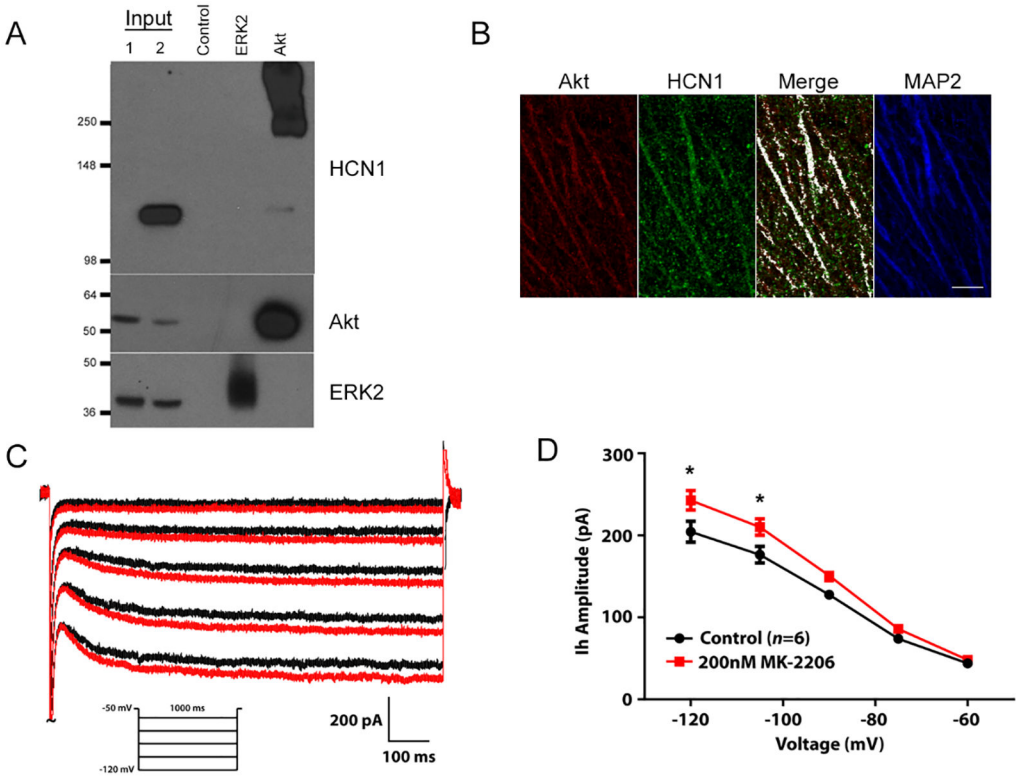

Figure 6.

A, HCN1 immunoreactivity detected in Akt IP from the hippocampus. Input 1 is 25μg solubilized starting material (i.e. total lysate) for the IP and Input 2 is 25μg of isolated membranes from the hippocampus. Hippocampal total lysate was immunoprecipitated with normal rabbit serum (i.e. control), ERK2 antibody, or an Akt antibody. The immunoblotting antibodies are indicated on the right of the immunoblots. **B**, Colocalization(white) of HCN1(green) and Akt(red) in the distal dendrites of the CA1 region of the hippocampus. MAP2 (blue) was used a dendritic marker. 63× magnification, scale bar = 10μM. **C**, The Akt inhibitor, MK-2206, increases Ih in CA1 neurons. Representative current traces (capacitance artifacts truncated) showing Ih relaxations obtained upon hyperpolarization (voltage protocol shown below recordings, detailed in the methods) Comparison of traces in control(black) and during superfusion of 200nM MK-2206 (red) revealed that MK-2206 increased the h-current relaxation. **D**, Peak Ih amplitude plotted against voltage for control (black circles) and after superfusion of 200nM or 500nM (both concentrations had similar effects and data were combined) MK-2206 for 12 minutes (red diamonds).*,p<0.05;Two-way ANOVA.